Figures and figure supplements

Motility precedes egress of malaria parasites from oocysts

Dennis Klug and Friedrich Frischknecht

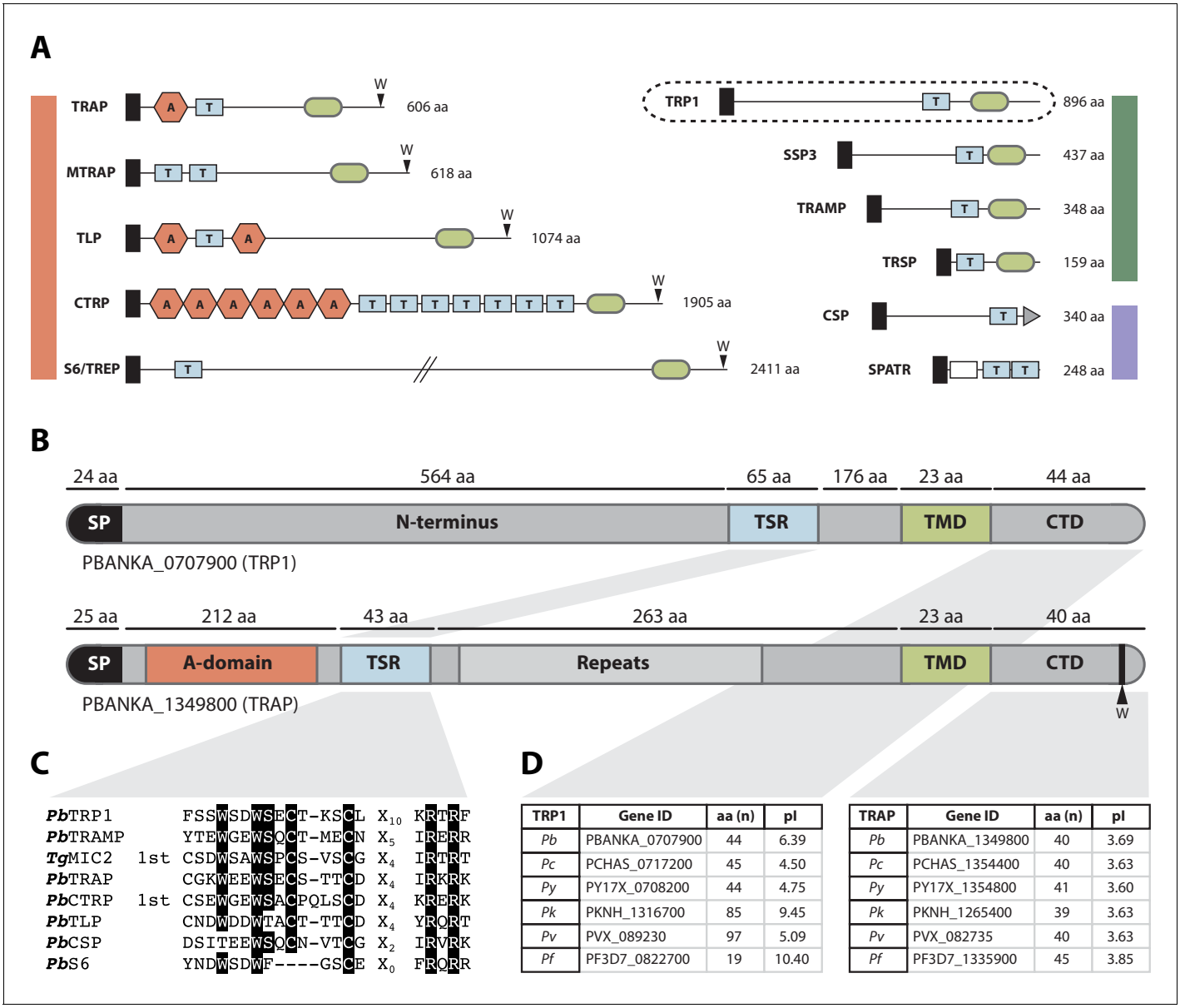

TRP1	Gene ID	aa (n)	pI
Pb	PBANKA_0707900	44	6.39
Pc	PCHAS_0717200	45	4.50
Py	PY17X_0708200	44	4.75
Pk	PKNH_1316700	85	9.45
Pv	PVX_089230	97	5.09
Pf	PF3D7_0822700	19	10.40

TRAP	Gene ID	aa (n)	pI
Pb	PBANKA_1349800	40	3.69
Pc	PCHAS_1354400	40	3.63
Py	PY17X_1354800	41	3.60
Pk	PKNH_1265400	39	3.63
Pv	PVX_082735	40	3.63
Pf	PF3D7_1335900	45	3.85

Figure 1. The thrombospondin-related protein 1 (TRP1) shares distinct domains with TRAP-family proteins, belongs to the family of TRAP-like proteins and is present in all *Plasmodium* species. (**A**) TSR-containing proteins in *Plasmodium*. TRAP-family proteins are marked with a red bar, whereas TRAP-related proteins are indicated by a green bar and other TSR-containing proteins by a blue bar. TRP1 is encircled by a dashed line (top right). Thrombospondin repeats are shown as blue boxes (labeled with T) and Von Willebrandt factor like A-domains are depicted as red hexagons (labeled with A). Signal peptides are shown as black boxes and transmembrane domains as light green ovals. CSP possesses a GPI-anchor (grey triangle), whereas SPATR harbors an EGF-domain (white box). Conserved tryptophans are indicated with a W. Protein schemes are not drawn to scale and amino acid numbers refer to *P. berghei* proteins. (**B**) Protein model of *Pb*TRP1 (PBANKA_0707900; 896 amino acids) in comparison to *Pb*TRAP (PBANKA_1349800, 606 amino acids, not to scale). Both proteins contain a signal peptide (SP), a thrombospondin type-I repeat (TSR), a transmembrane domain (TMD) and a cytoplasmic tail domain (CTD), but TRP1 lacks the conserved tryptophan (W) that is typically found at the C-terminus of TRAP-family proteins. Instead of the Von Willebrandt factor-like A-domain in TRAP, TRP1 contains a long N-terminal extension. (**C**) Multiple sequence alignment of the *Pb*TRP1 TSR with TSRs from the TRAP-family (*Pb*TRAP, *Tg*MIC2, *Pb*CTRP, *Pb*S6 and *Pb*TLP) and other TSR-containing proteins (*Pb*TRAMP and *Pb*CSP). (**D**) Length (in amino acids) and isoelectric point (pI) of the CTDs of TRP1 and TRAP from different *Plasmodium* species.
DOI: 10.7554/eLife.19157.003

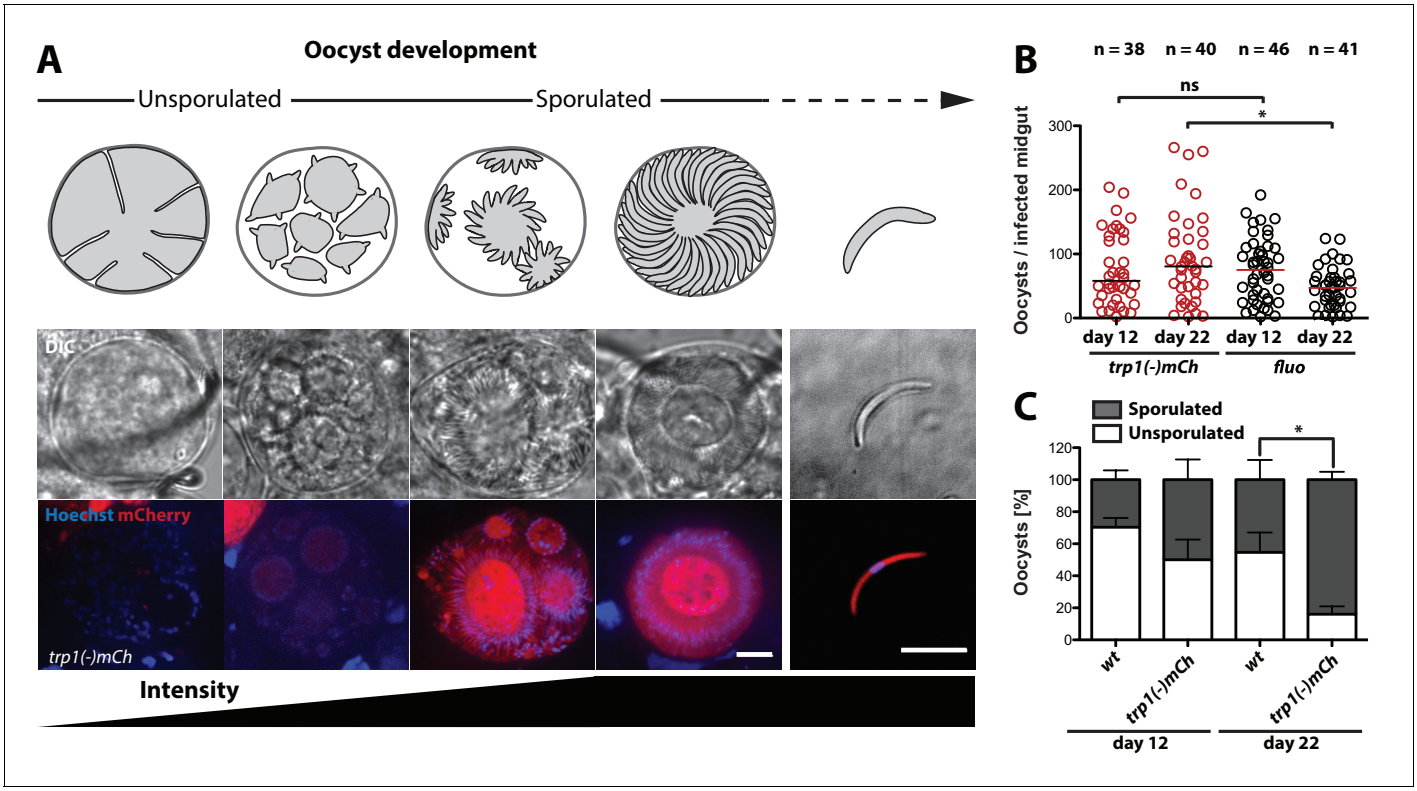

Figure 2. *trp1(-)* oocysts sporulate normally and persist in a sporulated state. (**A**) Expression of mCherry in *trp1(-)mCh* parasites was only observed in sporulating oocysts and sporozoites. The developmental stage of the oocysts is depicted schematically above the images, while the increase in fluorescence intensity is schematically indicated below. Strong mCherry expression was only observed in budding or mature oocysts. Scale bar: 10 μm. (**B**) Oocyst numbers of infected midguts for *trp1(-)mCh* and wild-type parasites at day 12 and day 22 post-infection. * depicts $p<0.05$; one-way ANOVA followed by a Kruskal-Wallis test. Horizontal bars indicate the median. Data were generated from two (*trp1(-)mCh*) and three (*fluo*) different feeding experiments, respectively. (**C**) Percentages of sporulated and unsporulated oocysts in *trp1(-)mCh* and wild-type infected midguts at 12 and 22 days post infection. * depicts $p<0.05$; one-tailed Student's t-test. The mean and the SEM are shown. Data were generated from three different feeding experiments.

DOI: 10.7554/eLife.19157.005

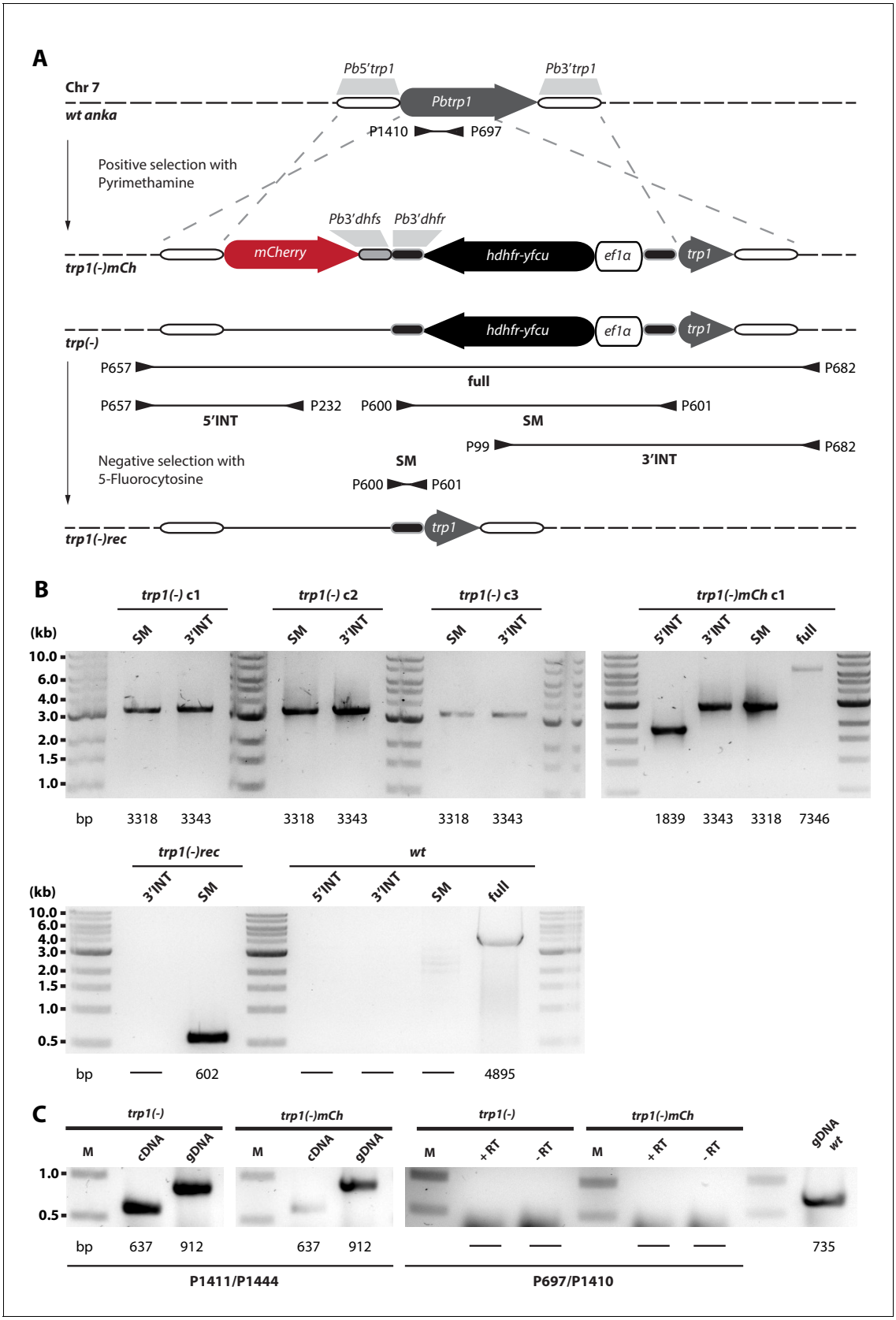

Figure 2—figure supplement 1. Generation and PCR analysis of *trp1(-), trp1(-)mCh* and *trp1(-)rec* parasites. (**A**) Schematic representation of the strategy for gene deletion and marker recycling via negative selection. Two different *trp1(-)* lines were generated by independent transfection of two

Figure 2—figure supplement 1 continued on next page

Figure 2—figure supplement 1 continued

different constructs into wild-type (*wt) P. berghei* strain ANKA parasites. The vector contained the positive-negative selection marker *hdhfr-yfcu*. The marker gene was flanked by ~1 kb sequences upstream and downstream of the open reading frame of *trp1* to generate a knockout line by double crossover homologous recombination (*trp1(-)).* In addition, a second vector was generated to visualize *trp1* promoter activity in vivo via expression of mCherry (*trp1(-)mCh*). Location of primers and the approximate length of the PCR fragments used for genotyping are indicated by arrows and lines below the scheme. (**B**) PCR analysis of clonal *trp1(-)* and *trp1(-)mCh* parasites. Note the shift in size of the complete locus (full) between *trp1(-)mCh* and *wt*. The expected sizes of the PCR products are indicated below. PCR analysis of negatively selected knockout parasites *trp1(-)rec* revealed loss of the selection cassette. Note the shift in size of the PCR product for the selection marker (SM) before and after negative selection. (**C**) RT-PCR with cDNA generated from *trp1(-)* and *trp1(-)mCh* midgut sporozoites. The PCR with the primers P1411/P1444 shows the presence of cDNA indicated by the loss of an intron and the shift in size of α-tubulin I. The PCR with the primers P697/P1410 is specific for *trp1*. An internal control with gDNA from the *P. berghei ANKA* strain is also shown to verify that the PCR worked. See also ***Figure 5***.

DOI: 10.7554/eLife.19157.006

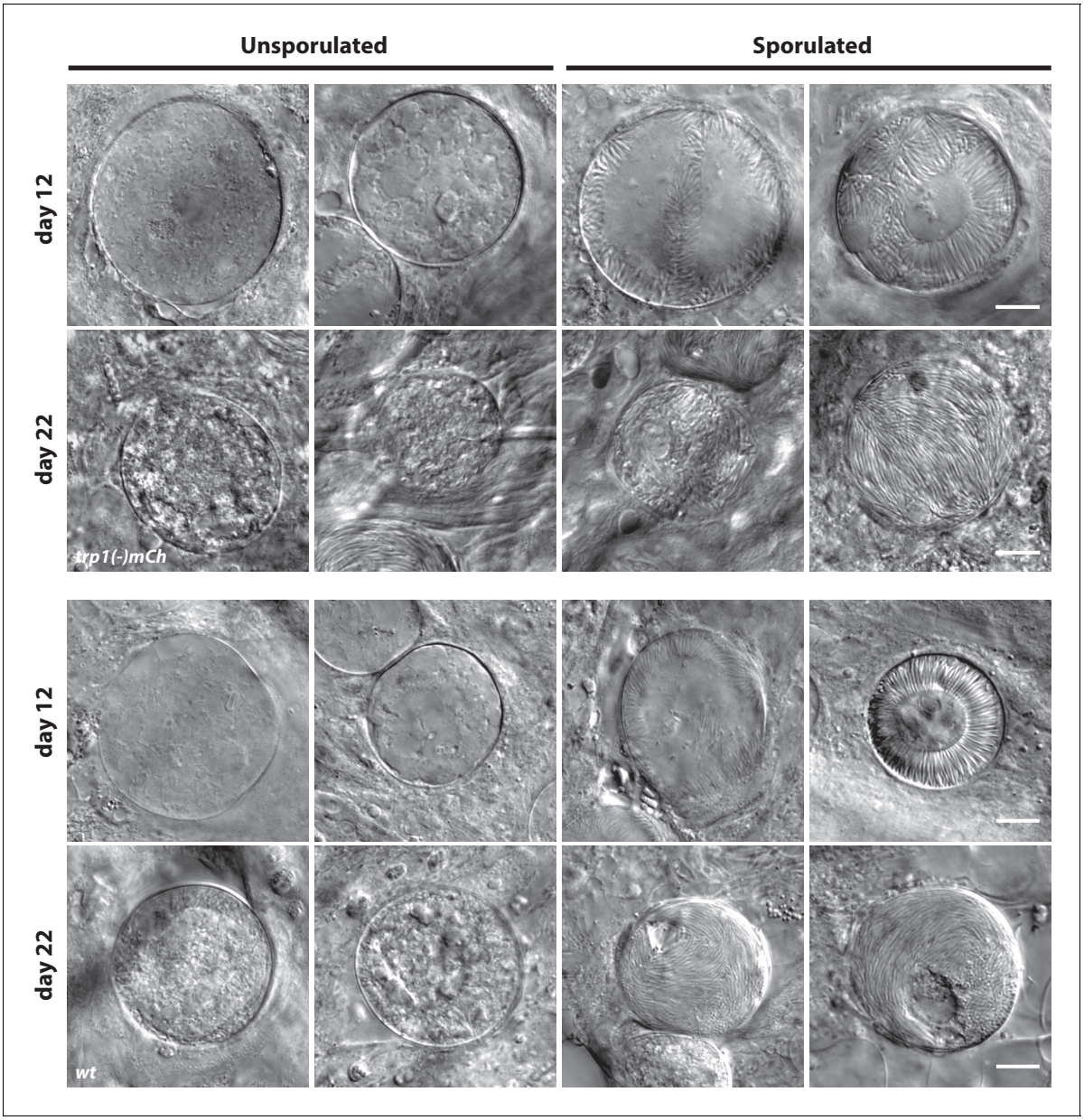

Figure 2—figure supplement 2. Classification of oocysts as unsporulated or sporulated. Examples of unsporulated and sporulated *trp1(-)mCh* and *wt* oocysts at day 12 and day 22. Note that oocysts with budding sporozoites as well as oocysts with completely developed sporozoites were classified as sporulated. Scale bar: 10 µm.

DOI: 10.7554/eLife.19157.007

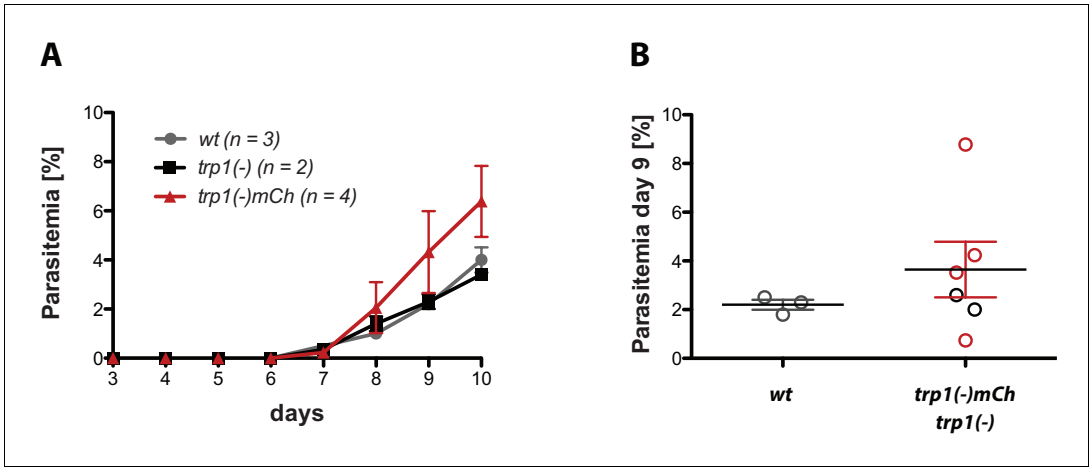

Figure 2—figure supplement 3. *trp1(-)* and *trp(-)mCh* midgut sporozoites are infective to mice if intravenously injected. (**A**) Midgut sporozoites of *trp1(-)* (400,000), *wt* (500,000) and *trp1(-)mCh* (500,000) were injected intravenously into four mice each. Parasitemia was monitored for 10 days post infection. Shown are the mean and SEM of four (*trp1(-)mCh*), two (*trp1(-)*) and three (*wt*) mice, which became blood-stage patent. (**B**) Parasitemia at day 9 post infection of the *wt*- and *trp1(-)mCh*-infected mice represented in (**A**).

DOI: 10.7554/eLife.19157.008

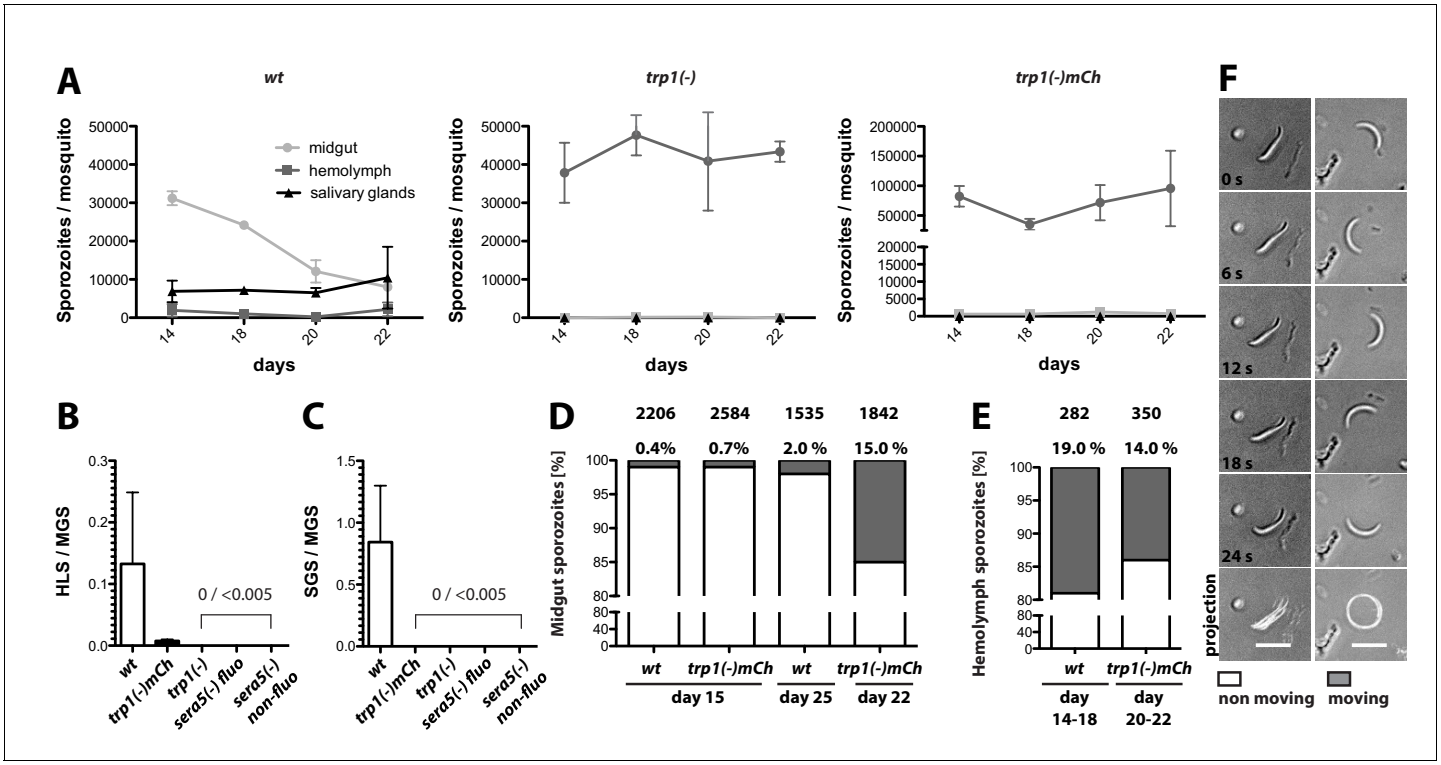

Figure 3. *trp1(-)* sporozoites are impaired in oocyst egress and salivary gland invasion but show normal gliding motility in vitro. (**A**) Numbers of wild-type, *trp1(-)* and *trp1(-)mCh* sporozoites in midguts, hemolymph and salivary glands over time. Shown are one to three countings per time point from one to three different feeding experiments. (**B**) Ratio of hemolymph (HLS) to midgut (MGS) sporozoites in wild-type-, *trp1(-)*- and *trp1(-)mCh*-infected mosquitoes. As negative control for a parasite that is not able to egress, a fluorescent and a non-fluorescent *sera5(-)* line were used. The bar represents the mean of four independent countings (ten mosquitoes each) at days 14, 17/18, 20 and 22 post infection of a selected feeding experiment. Error bars represent SEM. For absolute numbers see ***Table 2***. (**C**) Ratio of salivary gland (SGS) to midgut (MGS) sporozoites corresponding to (**B**).
The bar represents the mean, and error bars reflect SEM. For absolute numbers see ***Table 2***. (**D**) Percentage of moving (dark) and non-moving (white) midgut sporozoites of wild-type and *trp1(-)mCh* at the indicated days post infection. Sporozoites were classified as moving if they were able to glide for at least one full circle within five minutes. All sporozoites that behaved differently were classified as non-moving. The number of investigated sporozoites is indicated on top of the bars. (**E**) Percentage of moving (dark) and non-moving (white) hemolymph sporozoites of wild-type and *trp1(-)mCh*. (**F**) Example of a non-moving (floating, left column) and a moving (circular movement, right column) *trp1(-)mCh* sporozoite isolated from the hemolymph. Scale bar: 10 μm.
DOI: 10.7554/eLife.19157.009

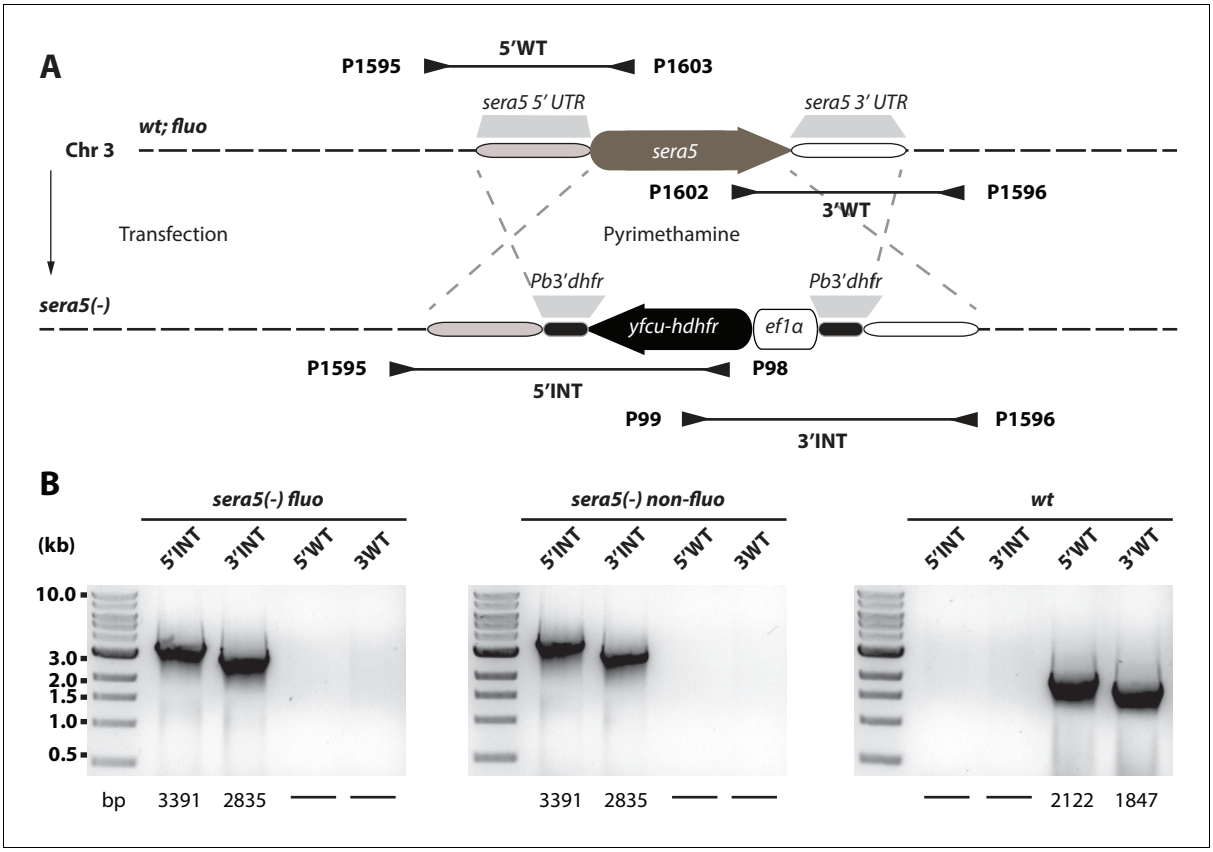

Figure 3—figure supplement 1. Generation and PCR analysis of *sera5(-) fluo* and *sera(5) non-fluo* parasites. Schematic representation of the *sera5* knockout strategy. (**A**) Two different *sera5(-)* lines were generated by two independent transfections, one into *wt* and one into the fluorescent-selection marker-free line *fluo*. The vector contained the positive-negative selection marker *hdhfr-yfcu*. The marker gene was flanked by ~1 kb sequences upstream and downstream of the open reading frame of *sera5* to generate a knockout line by double crossover homologous recombination. Positive transfections gave rise to two different lines named *sera5(-) fluo* and *sera5(-) non-fluo*. The location of primers and the approximate length of PCR fragments used for genotyping are indicated by arrows and lines below the scheme. (**B**) PCR analysis of clonal *sera5(-) fluo* and *sera5(-) non-fluo* parasites. The expected sizes of PCR products are indicated below the gel images.

DOI: 10.7554/eLife.19157.010

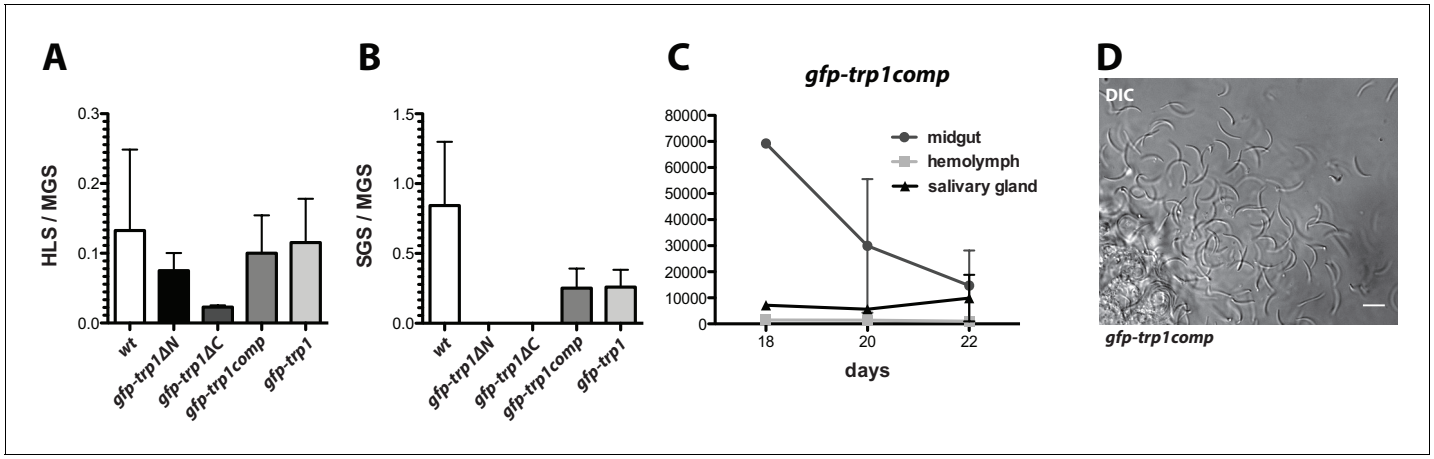

Figure 4. Complementation of *trp1(-)* parasites with full-length but not truncated TRP1 restores the wild-type phenotype. (**A**) Ratio of hemolymph sporozoites (HLS) to midgut sporozoites (MGS) and (**B**) of salivary gland sporozoites (SGS) to midgut sporozoites (MGS) for *gfp-trp1ΔN, gfp-trp1ΔC gfp-trp1comp* and *gfp-trp1* lines in comparison to wild-type (*wt*) parasites. The bar charts show the mean of four independent countings (10 mosquitoes each) at days 14, 18, 20 and 22 post infection of a selected feeding experiment. For absolute numbers see ***Table 2***. Error bars represent SEM. (**C**) Sporozoites of *gfp-trp1comp* in midguts, salivary glands and hemolymph counted over time; 1–2 countings per timepoint. (**D**) Mechanically ruptured salivary gland releasing *gfp-trp1comp* sporozoites. Scale bar: 10 μm.

DOI: 10.7554/eLife.19157.012

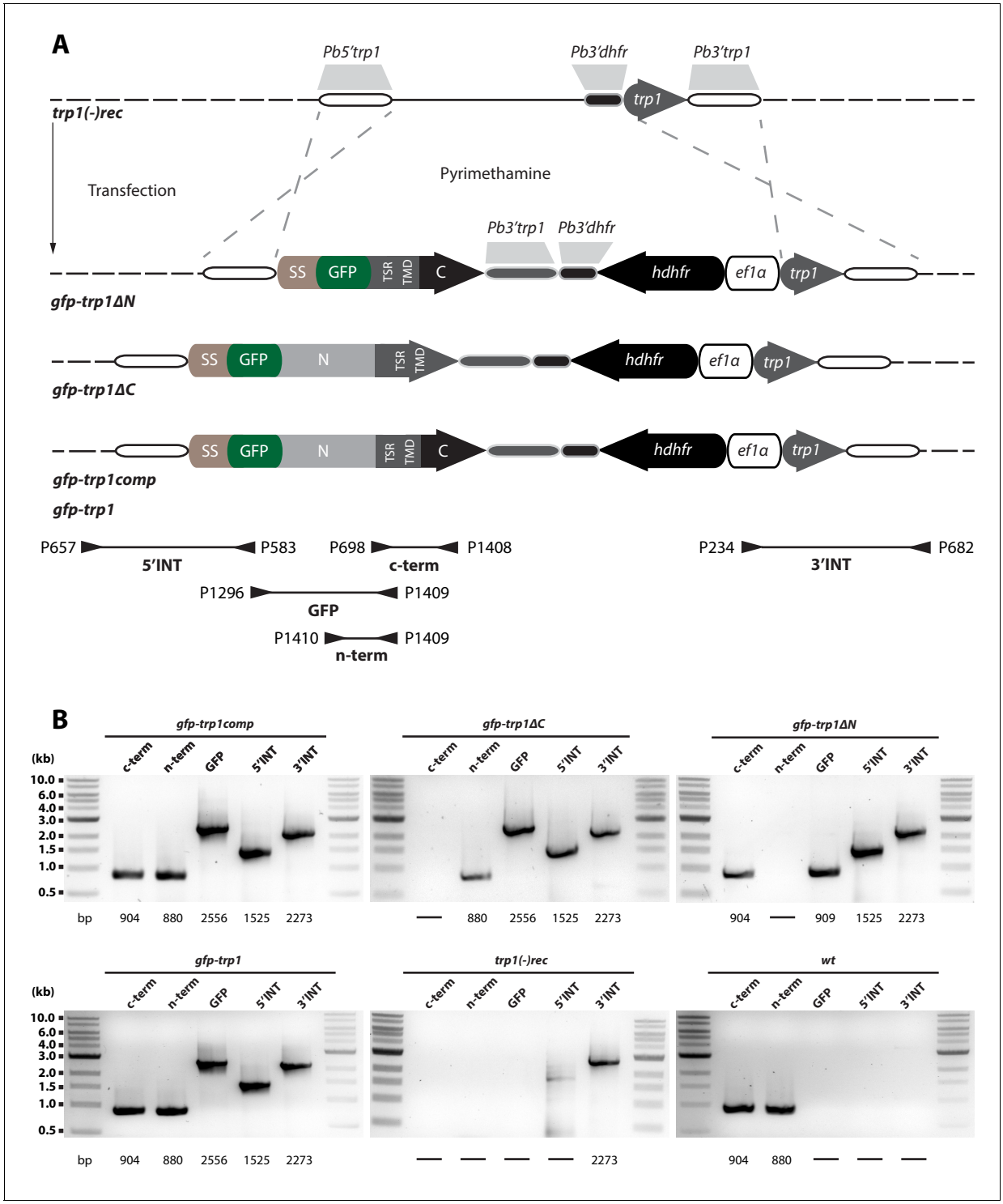

Figure 4—figure supplement 1. Generation and PCR analysis of *gfp-trp1comp*, *gfp-trp1*, *gfp-trp1ΔN* and *gfp-trp1ΔC* parasites. Schematic representation of the complementation strategy with sequences encoding full-length and truncated TRP1 proteins. (**A**) Complementation was performed with three different constructs (*gfp-trp1*, *gfp-trp1ΔN* and *gfp-trp1ΔC*). All constructs contained the positive selection marker *hdhfr* under control of the *ef1α* promoter and a *GFP* gene at the N-terminal end, between the sequence encoding the signal peptide and the remaining *trp1* ORF. The location of primers and the length of PCR fragments used for genotyping are indicated by arrows and black lines below the scheme. Approximate sizes of the PCR products are indicated below the images. (**B**) PCR analysis of clonal lines revealed correct integration of the designed constructs. To probe for the absence of deleted sequences, two PCRs specific for the N- and C-terminus of *trp1* (n-term and c-term) were performed. The PCR termed

Figure 4—figure supplement 1 continued on next page

Figure 4—figure supplement 1 continued

GFP amplifies a sequence between *GFP* and *trp1* to test the fusion of both sequences. For comparison, the PCRs for both recipient lines *trp1(-)rec* and *wt* are shown.

DOI: 10.7554/eLife.19157.013

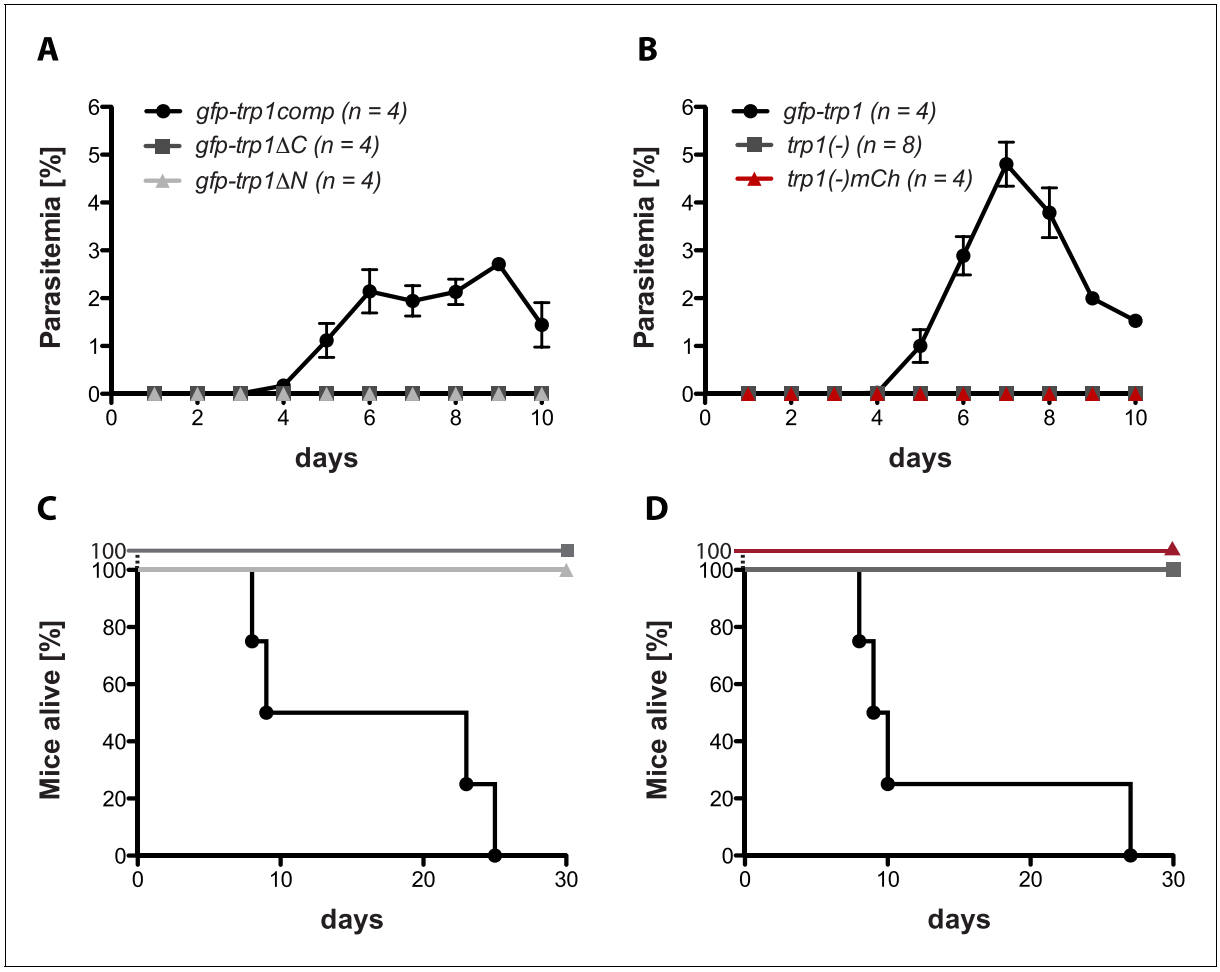

Figure 4—figure supplement 2. TRP1 is essential for transmission by infected mosquitoes. (**A**,**B**) Parasitemia in mice exposed to ten mosquitoes infected (**A**) with *gfp-trp1:comp*, *gfp-trp1ΔC* and *gfp-trp1ΔN* and (**B**) with *trp1(-)*, *trp1(-)mCh* and *gfp-trp1*. Blood stage parasites were monitored for 10 days post infection. The graphs show the mean and the standard error of the mean (SEM) of the parasitemia for all infected mice per group (n). (**C**,**D**) The survival of mice infected with *gfp-trp1comp*, *gfp-trp1ΔC* and *gfp-trp1ΔN* (corresponding to (**A**)) and with *trp1(-)*, *trp1(-)mCh* and *gfp-trp1* (corresponding to (**B**)). The viability of all mice was monitored for 30 days post infection.

DOI: 10.7554/eLife.19157.014

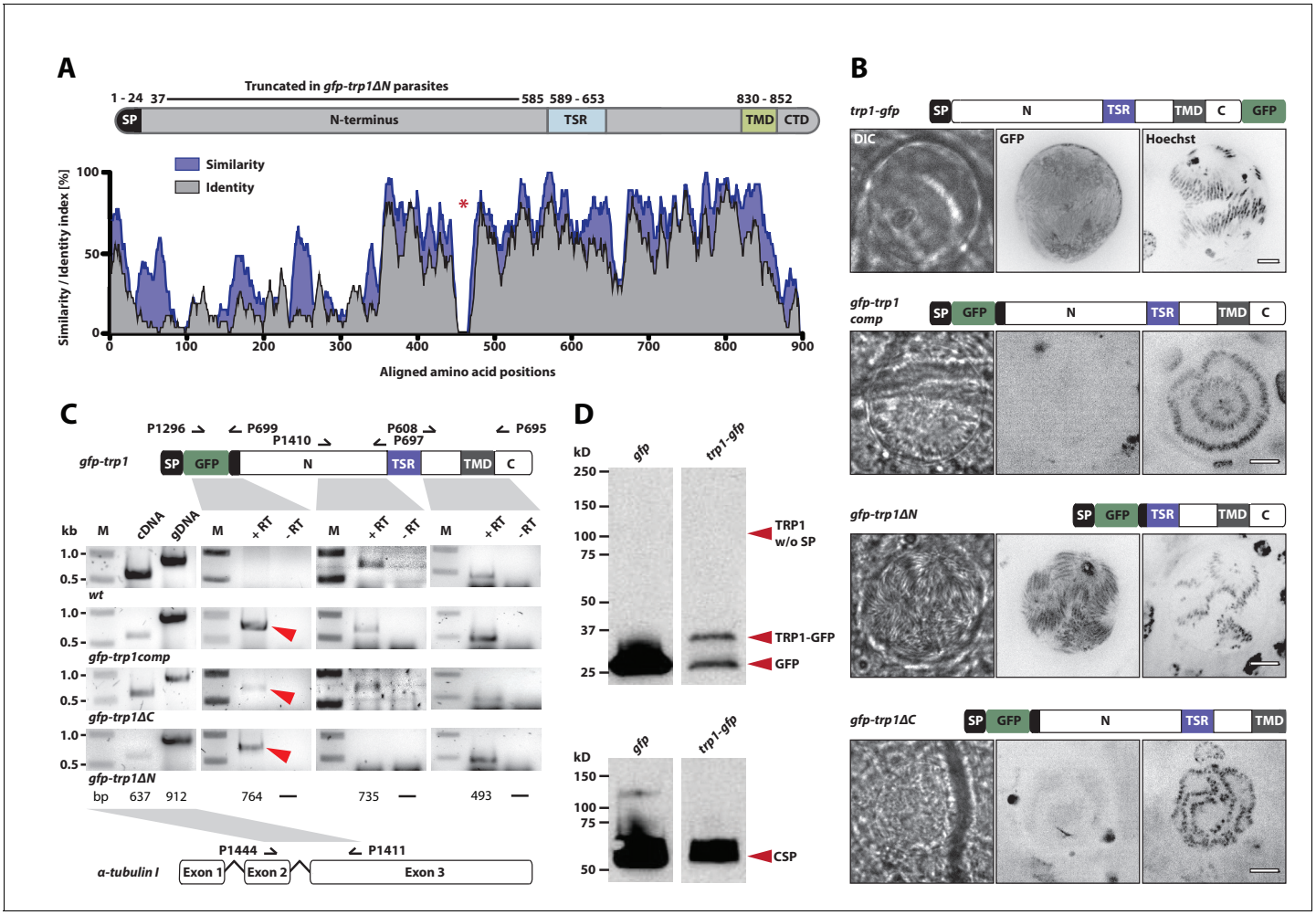

Figure 5. TRP1 is post-translationally processed. (**A**) Appearance of conserved residues (identity) and residues with similar charge (similarity) in *Pf*TRP1, *Pv*TRP1 and *Pk*TRP1 in reference to *Pb*TRP1. The graph corresponds to the protein model of TRP1 shown above. The gap marked by a red asterisk indicates an insertion in the sequence that is unique to *Pb*TRP1. Note the less conserved nature of part of the N-terminus. (**B**) Localization of TRP1-GFP, GFP-TRP1comp, GFP-TRP1ΔN and GFP-TRP1ΔC in oocysts 11–14 days post infection. Nuclear DNA is stained with Hoechst. Scale bar: 10 μm. See also ***Video 1***. (**C**) RT-PCR of cDNA generated from midgut sporozoites. Purity of cDNA was tested with α-tubulin I primers amplifying a sequence from exon 2 to exon 3 (left). Splicing of the intron in-between the two exons resulted in a smaller PCR fragment compared to the gDNA. A *gfp:trp1* fusion transcript could be detected in *gfp-trp1comp*, *gfp-trp1ΔN*, and *gfp-trp1ΔC* (indicated by red arrowheads) but not in *wt* sporozoites. In addition, two PCRs were performed to detect two different parts of the *trp1* transcript. The gene and protein models shown below and above the images are not drawn to scale. (**D**) Western blot with 100,000 *trp1-gfp* and *csgfp* midgut sporozoites. The two lanes below show as loading control CSP, while the bands above show signals for GFP. Sporozoites expressing TRP1-GFP show a band at ~26 kDa that corresponds to free GFP and a second band at ~35 kDa that corresponds to GFP fused to the C-terminus and the transmembrane domain of TRP1. The predicted size of untagged TRP1 after cleavage of the signal peptide (~104 kDa) is indicated by a red arrow. Note that the shown images correspond to the same blot that was exposed for the same time. Lanes in-between the shown samples were only removed to simplify the representation.

DOI: 10.7554/eLife.19157.015

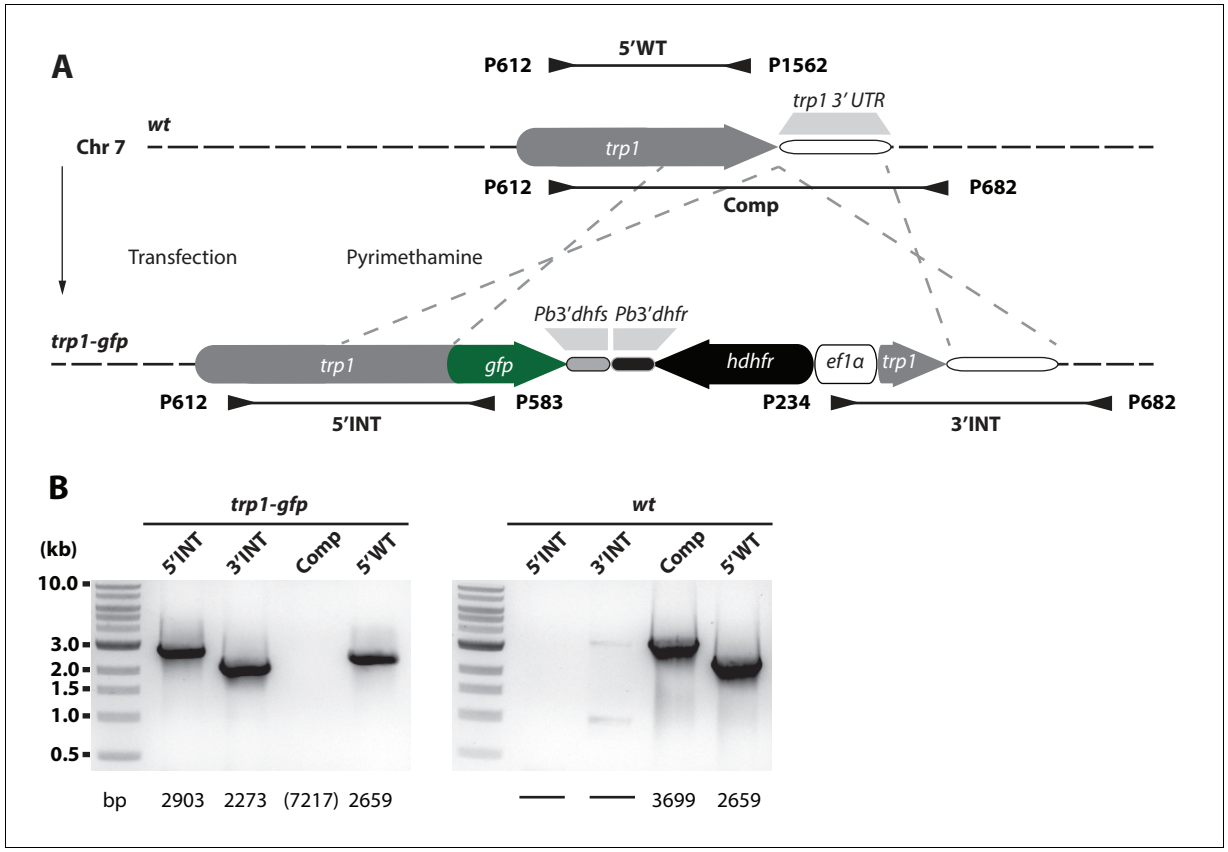

Figure 5—figure supplement 1. Generation and PCR analysis of parasites expressing TRP1 fused C-terminally to GFP (*trp1-gfp*). Schematic representation of the C-terminal tagging strategy for TRP1. (**A**) The line *trp1-gfp* was generated by transfection of *wt*. The vector contained the positive selection marker *hdhfr*, which was flanked by the C-terminal end of the TRP1 ORF and the TRP1 3'UTR. Integration of this sequence by double crossover homologous recombination resulted in a C-terminal fusion of TRP1 to GFP. Location of primers and approximate length of PCR fragments used for genotyping are indicated by arrows and lines below and above the scheme. (**B**) PCR analysis of clonal *trp1-gfp* and *wt* parasites. The expected sizes of PCR products are indicated below. Note that the PCR for the *trp1-gfp* line of the complete locus (Comp) could not be amplified, presumably because of the length and the high AT content of the sequence.

DOI: 10.7554/eLife.19157.016

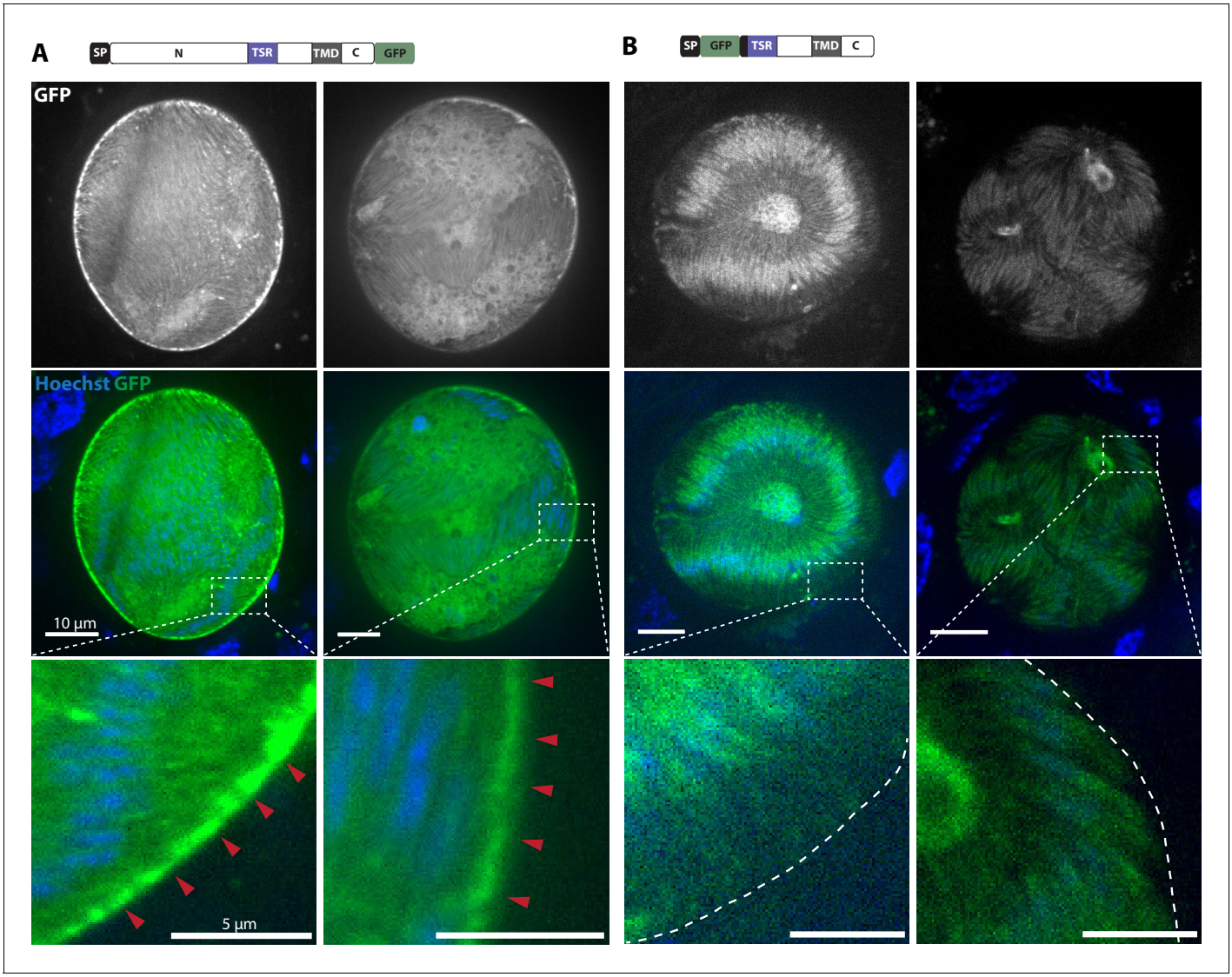

Figure 6. TRP1-GFP localizes to the oocyst wall while GFP-TRP1ΔN accumulates in the endoplasmatic reticulum (ER). (**A**) Localization of TRP1-GFP in oocysts 11–14 days post infection. Nuclear DNA is stained with Hoechst. The accumulation of GFP at the oocyst wall is indicated by red arrows in the zoomed images. See also ***Video 1***. (**B**) Localization of GFP-TRP1ΔN at 11–14 days post infection. Nuclear DNA is stained with Hoechst. The dashed white line in the zoomed images indicates the oocyst wall.

DOI: 10.7554/eLife.19157.018

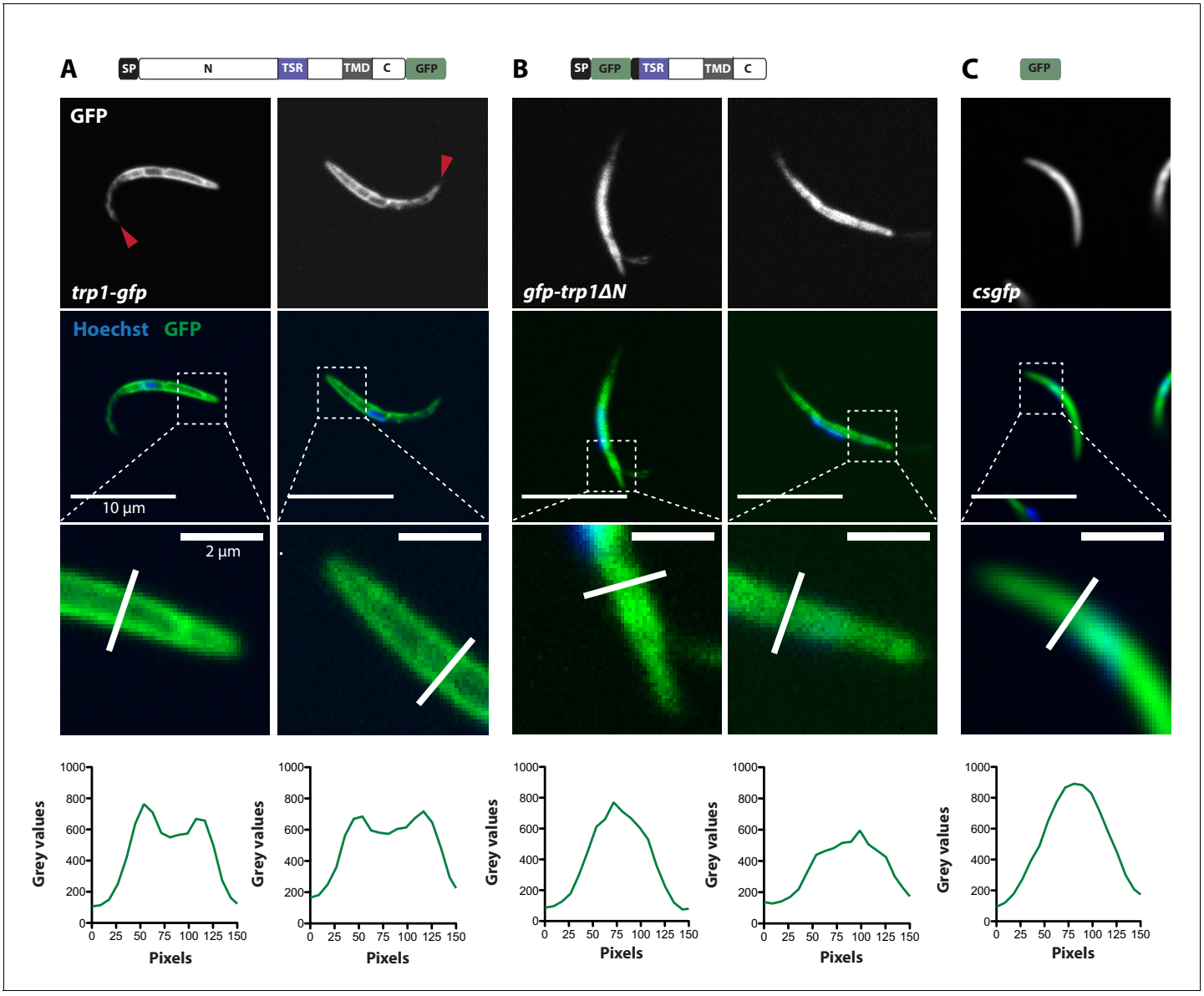

Figure 7. TRP1-GFP but not GFP-TRP1ΔN localizes in a polarized fashion at the sporozoite periphery. (**A**) Live imaging of hemolymph sporozoites expressing TRP1-GFP. The line plot below shows the intensity of grey values along the white line indicated in the zoomed image, showing the proximal end of the sporozoite. The GFP signal localizes close to the plasma membrane indicated by the intensity profile showing two peaks on both sides of the sporozoites. The red arrows point to the apical tip of the sporozoites. See also ***Video 2***. (**B**) Live imaging of midgut sporozoites expressing GFP-TRP1ΔN. The GFP signal is not equally distributed as seen in control parasites in (C) but does not localize close to the plasma membrane as shown in (A). (**C**) Live imaging of a salivary gland sporozoite expressing cytoplasmic GFP. In contrast to (A) and (B), the GFP signal is equally distributed within the cytoplasm.

DOI: 10.7554/eLife.19157.019

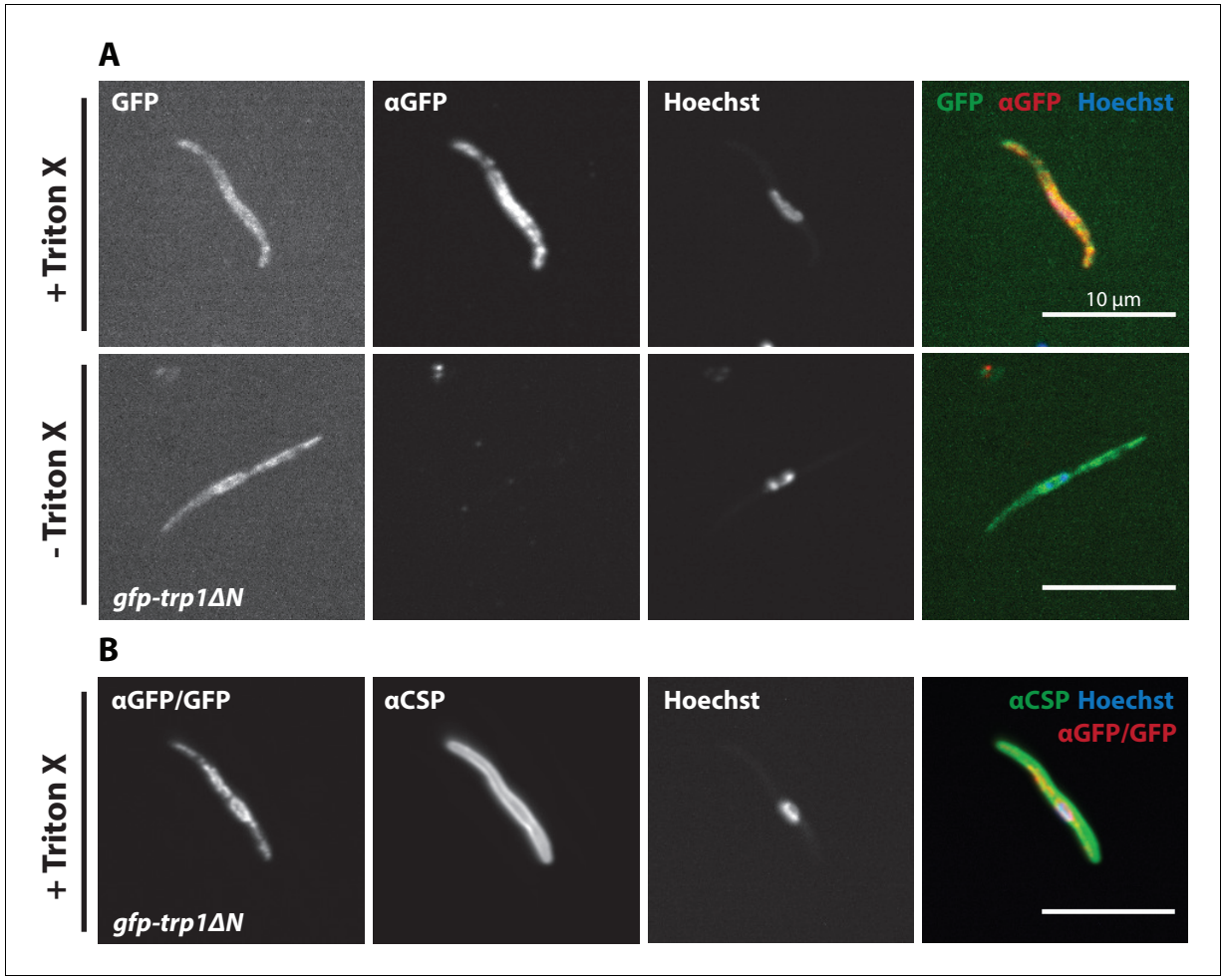

Figure 7—figure supplement 1. GFP-TRP1ΔN does not localize on the sporozoite surface. (**A**) Immunofluorescence of midgut sporozoites against GFP in the presence and absence of Triton-X 100. Note the absence of anti-GFP signal in the unpermeabilized sporozoite, suggesting that the GFP-TRP1ΔN fusion protein localizes within the sporozoite and not on the plasma membrane. (**B**) Positive control with antibodies against CSP, visualizing the plasma membrane.

DOI: 10.7554/eLife.19157.020

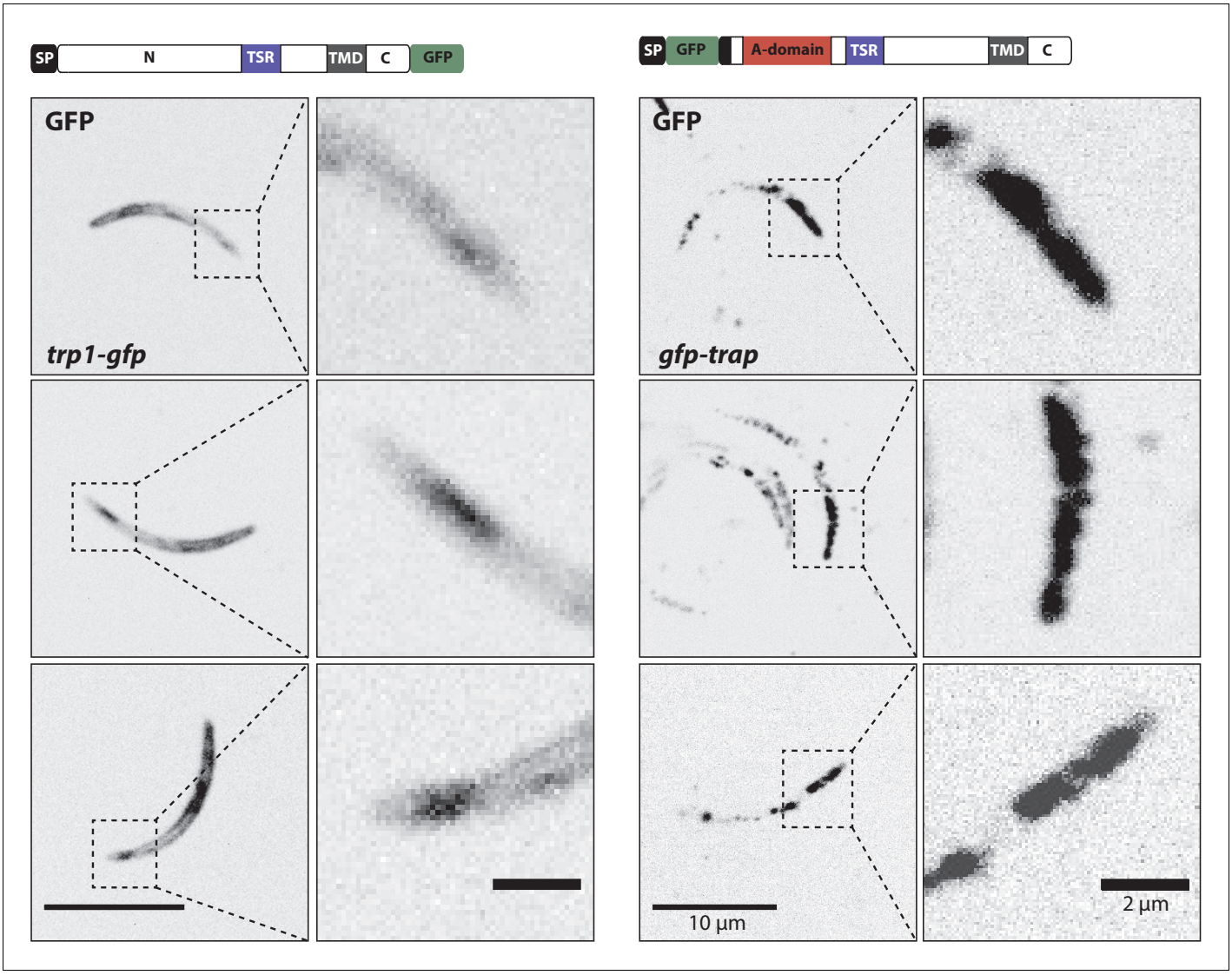

Figure 8. Localization of TRP1-GFP and the micronemal protein TRAP. Comparison of salivary gland sporozoites expressing C-terminally tagged TRP1 (*trp1-gfp*) with salivary gland sporozoites expressing N-terminally tagged TRAP (*gfp-trap*). Zoomed images all show the apical tip of the sporozoites. Three different sporozoites are displayed for each strain. While TRAP shows a micronemal localization, predominantly at the apex of the sporozoite, TRP1 localizes close to the plasma membrane and accumulates at the rear end of the sporozoite.

DOI: 10.7554/eLife.19157.021

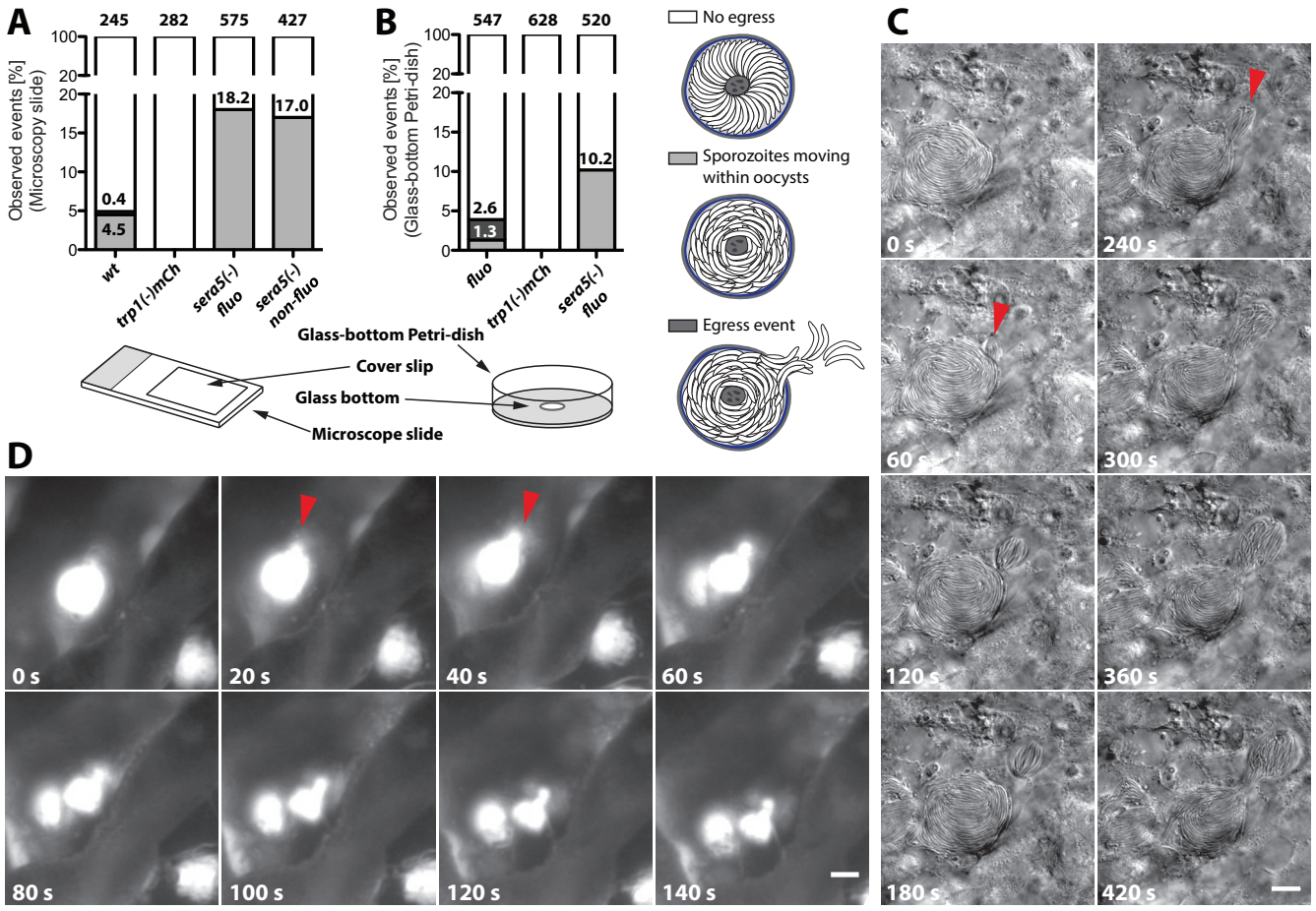

Figure 9. *trp1(-)* sporozoites do not egress from oocysts and do not show intra-oocyst motility. (**A**) Distribution of egress events (dark grey) and oocysts containing motile sporozoites (light grey) in control (*fluo*), wild-type (*wt*) or *sera5(-)* and *trp1(-)mCh* oocysts on a microscope slide covered with a cover slip or (**B**) uncovered in a glass-bottom Petri-dish. As control for a non-egressing strain, a fluorescent (*sera5(-) fluo*) and a non-fluorescent (*sera5(-) non-fluo*) SERA5 knockout line were tested. The different sample preparation methods are depicted below the graphs. Sporozoites budding from oocysts in a sporosome-like manner as well as spontanous bursting of oocysts were classified as egress events (***Videos 4–6***). (**C**) Time lapse of a budding event under a cover slip. A wild-type oocyst with budding sporozoites is shown. The start of two budding events is indicated with red arrows. Scale bar: 10 µm. See also ***Video 3***. (**D**) Bursting of an oocyst in a glass-bottom Petri-dish. An oocyst expressing GFP bursting and releasing sporozoites is shown. Scale bar: 20 µm. See also ***Video 7***.

DOI: 10.7554/eLife.19157.024

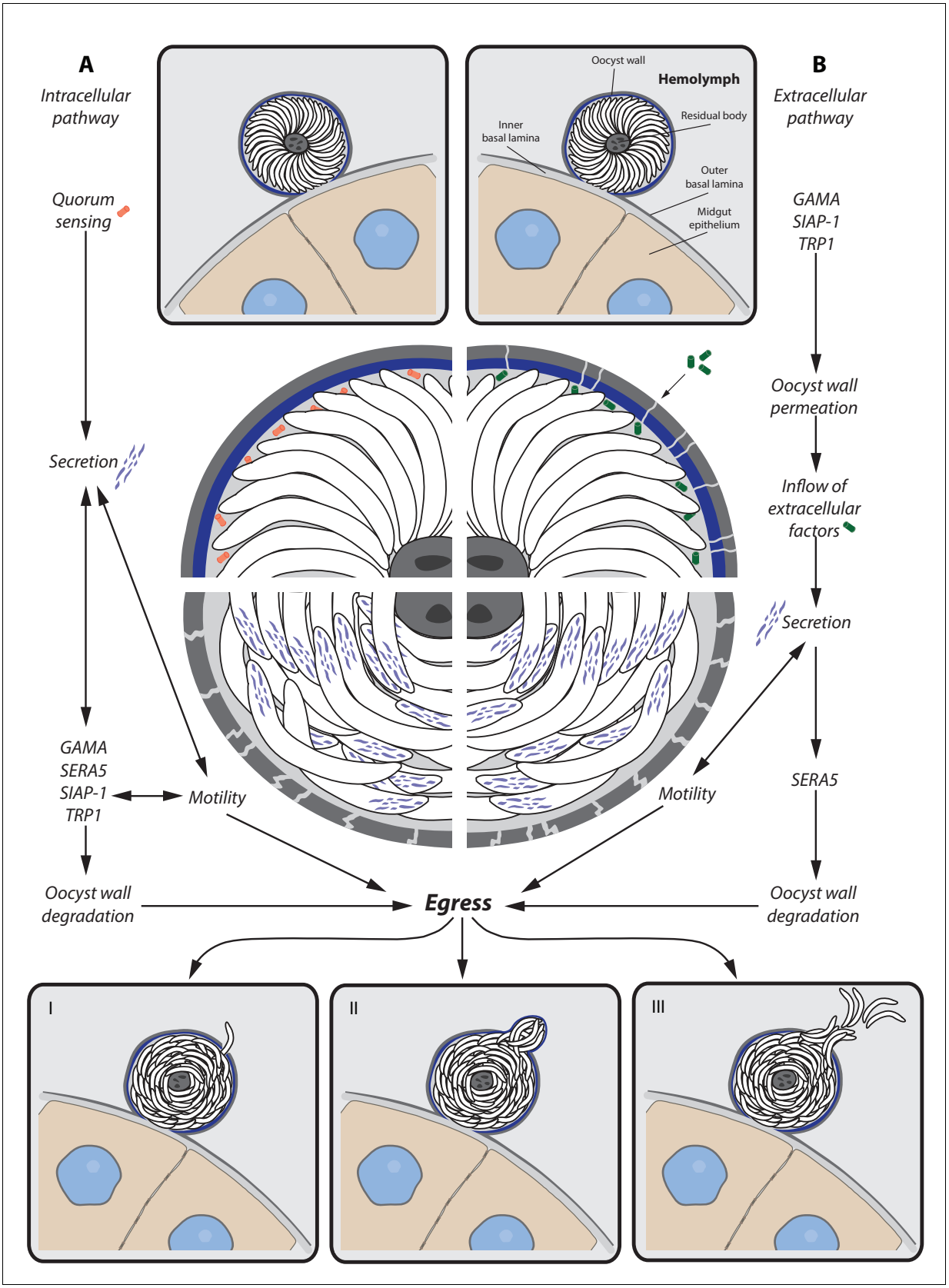

Figure 10. Potential model for sporozoite egress from oocysts. Hypothetical model of a cascade of events that lead to sporozoite egress from oocysts. (**A**) Intracellular pathway — possible quorum sensing between sporozoites leads to secretion of proteins (e.g. GAMA, SERA5, SIAP-1, TRP1) that trigger

Figure 10 continued on next page

Figure 10 continued

gliding motility and degradation of the oocyst wall, which is followed by sporozoite egress. (**B**) Extracellular pathway — expression of factors (e.g. GAMA, TRP1, SIAP-1) leads to permeabilization of the oocyst wall and inflow of extracellular factors. Inflowing factors trigger secretion of proteins that not only activate gliding motility but also degrade the oocyst wall (e.g. SERA5), which is followed by sporozoite egress. Egress of sporozoites can occur in different ways. (I) Single sporozoite egress — sporozoites migrate through thin holes in the oocyst envelope. (II) Sporosome formation — many sporozoites stretch the oocyst wall, leading to the formation of sporozoite filled vesicles (sporosomes) that bud from the oocyst. (III) Bursting oocyst — rapid rupture of the oocyst wall.

DOI: 10.7554/eLife.19157.031

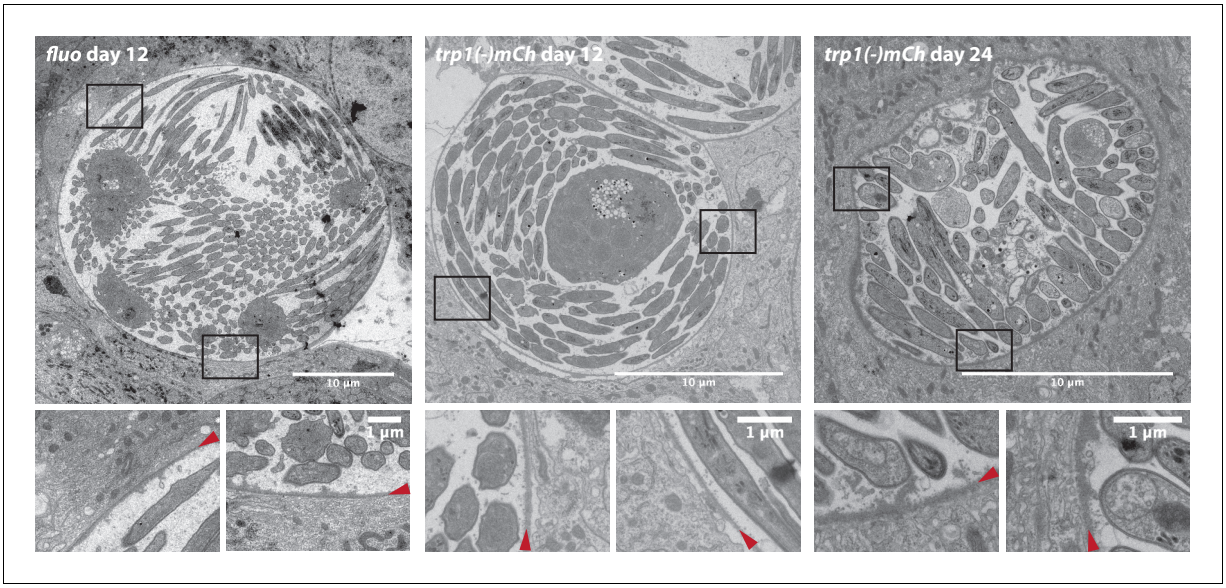

Figure 10—figure supplement 1. Electron microscopy of control (*fluo*) and *trp1(-)mCh* oocysts. Full midguts of the respective parasites were fixed 12 or 24 days post infection and processed for electron microscopy. Two focus sections of each oocyst illustrate the integrity of the oocyst wall indicated by red arrowheads. Scale bars are depicted within the images.

DOI: 10.7554/eLife.19157.032